Study on Capacitance Evolving Mechanism of Polypyrrole during Prolonged Cycling

ARTICLE *in* THE JOURNAL OF PHYSICAL CHEMISTRY B · JANUARY 2014

Impact Factor: 3.3 · DOI: 10.1021/jp4054428 · Source: PubMed

6 AUTHORS, INCLUDING:

Youlong Xu
Xi'an Jiaotong University
78 PUBLICATIONS **1,049** CITATIONS
SEE PROFILE

Jie Wang
Stanford University
612 PUBLICATIONS **12,030** CITATIONS
SEE PROFILE

Yang Bai
Xi'an Jiaotong University
8 PUBLICATIONS **36** CITATIONS
SEE PROFILE

Lilong Xiong
Xi'an Jiaotong University
15 PUBLICATIONS **119** CITATIONS
SEE PROFILE

THE JOURNAL OF PHYSICAL CHEMISTRY B

Article

pubs.acs.org/JPCB

Study on Capacitance Evolving Mechanism of Polypyrrole during Prolonged Cycling

JingPing Wang,*[,†,‡] Youlong Xu,*[,‡] Jie Wang,[‡,§] Jianbo Zhu,[‡,§] Yang Bai,[‡,§] and Lilong Xiong[‡,§]

[†]College of Chemistry and Chemical Engineering, Shaanxi University of Science and Technology, Xi'an 710021, China

[‡]Electronic Materials Research Laboratory, Key Laboratory of the Ministry of Education, Xi'an Jiaotong University, Xi'an 710049, China

Supporting Information

ABSTRACT: A simple model on the evolution mechanism of PPy capacitance during prolonged cycling offers a reasonably description on the rapid increase and decay of PPy capacitance in 1 M 1-ethyl-3-methylimidazolium tetrafluoroborate/propylene carbonate ($EtMeImBF_4$/PC). The capacitance of PPy films reached a very high specific capacitance of 420 $F{\cdot}g^{-1}$ after 15 cycles when they worked in 1 M $MeEt_3ImBF_4$/PC. However, the capacitance rapidly decreased to 5% after only 400 cycles. The electronic conductivity and protonation level on the nitrogen site of PPy films rapidly decreased with the increase of cyclic number. The salt of $EtMeImBF_4$ was monitored in PPy matrix by FTIR spectra after 400 cycles. The EQCM results indicated that a lot of 1-ethyl-3-methylimidazolium cations ($EtMeIm^+$) were inserted during reduction process and retained in PPy matrix. The detained $EtMeIm^+$ cations bonded with doped *p*-toluenesulfonate anions (PTS^-) in PPy matrix or BF_4^- anions from electrolyte and formed salts. Small amount of salts in PPy matrix can open more channels of ion insertion and resulted in a very high capacitance after 15 cycles. The continuous combination of detained $EtMeIm^+$ cations with doping anions of PTS^- resulted in the rapid decrease of PPy protonation level on the nitrogen site and formation of compensate semiconductor state in PPy matrix. This should be responsible for the rapid decay of PPy conductivity and capacitance. The continuous accumulation of salts resulted in the great increase of PPy internal resistance.

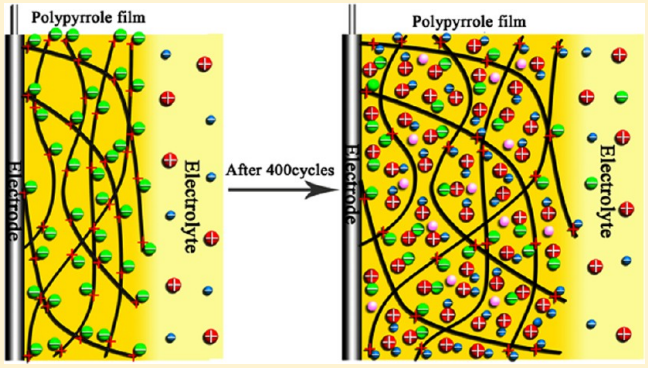

1. INTRODUCTION

Polypyrrole (PPy) is considered as one of most potential materials for several applications, including batteries, supercapacitors, electrochemical sensors, artificial muscles, electromagnetic interference shielding, antistatic coatings, and drug delivery systems, due to its high electronic conductivity, long-term environmental stability, environmental friendliness, and the relatively easy synthesis process.[1−4] However, the irreversible electrochemical process often occurred in PPy matrix at high anodic potentials and resulted in a rapid decay of PPy capacitance and electronic conductivity.[5−8] Much attention has been devoted to improving the stability of PPy.[2,9−12]

The mechanism of PPy irreversible electrochemical process should be very important to improve the PPy stability further in various electrolytes. Up to now, most published research on PPy irreversible electrochemical process focused on the mechanism of PPy degradation.[13−19] The overoxidation of PPy ring was considered as one of main reasons for PPy degradation in various electrolytes.[13] Bard et al.[17] first found that overoxidation of PPy occurs at potentials in excess of 0.6 V versus saturated calomel electrode. Later, Beck et al.[18] studied the effect of nucleophiles (such as OH^-, Br^-, etc.) on PPy overoxidation and presented the mechanism of PPy overoxidation. The overoxidation interrupts conjugate structure at PPy backbone due to the formation of hydroxyl and carbonyl groups, as well as the formation of CO_2 at very positive potentials.[20] The doped anions are expelled from PPy matrix during the process of overoxidation, which should reduce the doping level and electronic conductivity of PPy. The overoxidation of PPy is closely related to its working conditions.[21] Li et al.[21] found the higher the pH value, the lower the overoxidation potential will be, i.e., the easier the occurrence of the overoxidation, which is coincident with the electrolysis reaction of water to give out oxygen. Rodrigure et al.[20] investigated PPy overoxidation in aqueous KNO_3, KCl, and KF solutions and found that the overoxidation process of PPy occurred at less positive potential in F^- solution due to nucleophilic attack of OH^- ions originating from dissociation of the aqueous solvent.

The repeated redox cycles can damage PPy molecule structure and promote PPy degradation, leaving many pits and grooves on the surface of PPy.[22] The cations in working

Received: June 3, 2013
Revised: December 19, 2013
Published: January 15, 2014

   dx.doi.org/10.1021/jp4054428 | J. Phys. Chem. B 2014, 118, 1353−1362

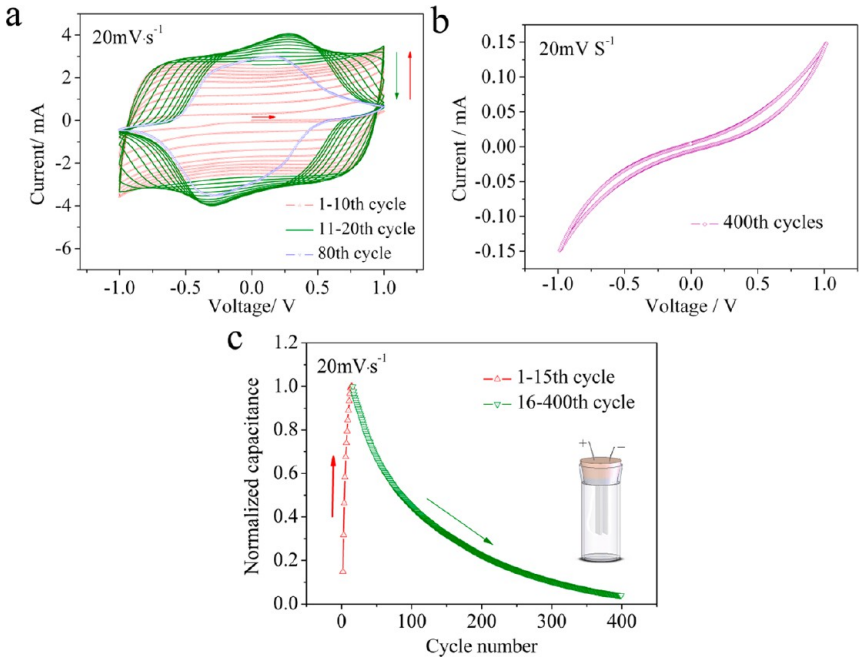

Figure 1. Cyclic voltammograms and capacitance decay curves of PPy films in two electrodes cell at a scan rate of 20 $mV{\cdot}s^{-1}$ in 1 M $EtMeImBF_4$/PC: (a) CV curves of PPy films from 1st to 80th cycles, (b) CV curve of PPy films after 400 cycles, and (c) the capacitance decay of PPy films from 1st to 400th cycles.

electrolyte have an important effect on PPy degradation. Our study has found the smaller cations in electrolyte solution can contribute to higher stability of PPy.[22] The smaller cations can result in smaller change of PPy volume during redox process, which might be the main reason for the high stability of PPy films in HCl aqueous solutions. Moreover, Marchesi et al.[16] investigated the degradation of PPy in aqueous $LiClO_4$ using electrochemical impedance spectroscopy (EIS) and found the huge increase in the charge transfer resistance. They considered that rigid islands entrapped by cross-linking points might be formed and thereby hinder the ionic interchange, which also resulted in the rapid decay of PPy specific capacitance.[7,16]

However, in this work, we offered a model on the rapid increase and decay of PPy capacitance in 1 M 1-ethyl-3-methylimidazolium tetrafluoroborate/propylene carbonate ($EtMeImBF_4$/PC) during prolonged cycling. The results of electrochemical quartz crystal microbalance (EQCM) indicated that the cations from supporting electrolyte can bond with the doped anions or the anions from supporting electrolyte and formed salts in PPy matix during the redox process. Small amount of salts in PPy matrix can open more channels of ion insertion and resulted in a very high capacitance of 420 $F{\cdot}g^{-1}$ after 15 cycles. The continuous combination of 1-ethyl-3-methylimidazolium cations ($EtMeIm^+$) with doping ions of p-toluenesulfonate anions (PTS^-) induced the formation of the compensate semiconductor state in PPy matrix. The rapid degradation of PPy films should be closely related to the formation of the compensate semiconductor state in PPy matix.

2. EXPERIMENTAL SECTION

2.1. Starting Materials. Pyrrole (Fluka, 99%) was distilled prior to use and stored at −10 °C in a nitrogen atmosphere. The working electrolyte in supercapacitors cells was the solution of 1 M $EtMeImBF_4$/acetonitrile ($EtMeImBF_4$/ACN) and 1 M $EtMeImBF_4$/PC (Shenzhen Capchem Technology Co., Ltd.). All other chemical reagents were used as received.

2.2. Electrode Preparation. The polymerization of PPy was carried out in aqueous solution containing 0.1 M pyrrole, 0.1 M *p*-toluenesulfonate acid (PTSA), and 0.3 M sodium *p*-toluenesulfonate (PTSS). A two-electrode electrochemical system was used for all polymerizations. The working electrode was a polished tantalum sheet with a surface area of 1 cm × 1 cm and the counter electrode was a Pt sheet with a surface area of 2 cm × 2 cm. The polymerization was performed by direct current and the current density was 1 $mA{\cdot}cm^{-2}$. The polymerization charge was 0.9 $C{\cdot}cm^{-2}$. All polymerizations were performed in an ice−water bath.

2.3. Characterization and Measurements. The morphology of PPy films was examined by field emission scanning electron microscope (FESEM, Hitachi, S-4800). The two-electrode supercapacitors cells after 50 cycles and 400 cycles were let standing for 20 min under the open circuit potential of 0 V for a steady electrochemical state before PPy films were taken apart from the cells for all tests. The electronic conductivities of PPy films were measured by a four point probe resistivity meter (Guangzhou 4-Probe Test, RTS-9) at 23 ± 1 °C. The PPy films for conductivity measurement were polymerized by the growth charge of $3C{\cdot}cm^{-2}$. Fourier transform infrared spectroscopy (FTIR) measurements (Bruker, VERTEX 70) were used to ascertain the chemical nature of PPy films. The sample of 1 mg PPy for FTIR measurement was typically examined in KBr pellets after thorough mixing. X-ray photoelectron spectroscopic (XPS) measurements were performed with an AXIS ultra DLD by Kratos Analytical Limited (Al Ka X-ray source, 1486.60 eV). All binding energies were referenced to the C 1s neutral carbon peak set at 284.6 eV to compensate for surface charging effects. The PPy films for FESEM, XPS and conductivity measurements were washed with alcohol and water before they were dried.

Two-electrode supercapacitors cells were assembled with two 1 cm × 1 cm PPy electrodes in dry argon glovebox, and the

dx.doi.org/10.1021/jp4054428 | J. Phys. Chem. B 2014, 118, 1353−1362

distance between two electrodes was 2 mm. The cells were airtight during prolonged cycling test of PPy films. All electrochemical tests were performed on the Versatile Multichannel Potentiostat 2/Z (VMP2, Princeton Applied Research). The cells were let standing for 20 min before every electrochemical test for a steady electrochemical state. In EQCM (Priceton Applied Research, QCM922) studies, a two-electrode system was used, with a gold film of 0.2 cm^2 on a 9 MHz AT-cut quartz crystal as the working electrode and a gold plate of 0.2 cm^2 as the counter electrode. The polymerization charge of PPy on the working electrode and counter electrode was both 0.9 $C{\cdot}cm^2$ in EQCM test. EIS measurements were carried out in three-electrode system, with a Pt plate of a 2 cm ×2 cm surface area as the counter electrode and an Ag wire in 0.01 $AgNO_3$/Acetonitrile with double junction as the reference electrode. EIS measurements were performed at 0 V in the frequency range from 10^5 Hz down to 10^{-2} Hz, using an ac amplitude of 10 mV.

3. RESULTS AND DISCUSSION

Figure 1 shows CV and capacitance decay curves of PPy films in 1 M EtMeImBF$_4$/PC. The capacitance and current of PPy films increased gradually in the first several cycles. PPy films prepared in aqueous solution are dense, suggesting that only the electrochemical response of the outer layers is being recorded in the first several cycles. The swelling of the PPy films occurred in EtMeImBF$_4$/PC and resulted in more active material participating in the redox process when the cyclic number increased further.[23] The specific capacitance of PPy films reached the maximum value of 420 $F{\cdot}g^{-1}$ after 15 cycles, which is higher than most published results.[2,10,11,22,24] Unfortunately, the specific capacitance began to decrease from 16th cycle and decreased to 5% of the maximum value after 400 cycles. Meanwhile, the shape of CV curves for PPy films varied dramatically during the degradation process of PPy films. It shows approximate rectangle before 10th cycle, and then the beak shape at tow ends of CV curves appears gradually from the 11th cycle. As shown in Figure 1b, the CV curve of PPy films is like that of pure resistance after 400 cycles, indicating that few ions participated in the doping/dedoping process of PPy films after 400 cycles. The similar results were obtained when PPy films worked in 1 M EtMeImBF$_4$/ACN, which was shown in Supporting Information. Table 1 lists the electronic conductivity of PPy films in 1 M EtMeImBF$_4$/PC at different degradation stages. The electronic conductivity decreased greatly with the increase of cyclic number and decreased by 2 orders of magnitude after 400 cycles. The rapid decay of the capacitance and electronic conductivity of PPy films should be related to the change of the PPy molecule structure.

Table 1. Electronic Conductivity of PPy Films in 1 M EtMeImBF$_4$/PC

PPy films	conduction ($S{\cdot}cm^{-1}$)
as-prepared PPy films	76−100
PPy films after 50 cycles	11−15
PPy films after 400 cycles	0.3−0.7

As shown in Figure 2a, PPy films prepared by direct current exhibit the typical "cauliflower" structures with large rises and falls (fluctuations) in the surface morphology.[11,23] PPy films in Figure 2, parts b and c, exhibit a more homogeneous and smoother appearance after 50 cycles and 400 cycles, which is consistent with the results in the Supporting Information. It is obvious that PPy films with more cyclic numbers resulted in a more homogeneous surface. Furthermore, there are a few fine cracks on the surface of PPy films after 400 cycles. In our previous works,[22] we found the surface of PPy films showed many pits and grooves when they were worked in 3 M KCl aqueous solution. It seems the surface of PPy films was not damaged seriously during the redox process in 1 M EtMeImBF$_4$/PC.

However, the thickness of PPy films changed dramatically with the increase of cyclic number for PPy films in Figure 3. The thickness of the as-prepared PPy films ranged from 1 to 1.5 μm. The thickness of PPy films increased and ranged from 1.5 to 2.0 μm after 50 cycles, and that increased more and ranged from 3.0 to 4.0 μm after 400 cycles, which reached about three times of its initial thickness. On the other hand, the cross section of PPy films became smoother after 50 and 400 cycles due to the disappearance of fold on the cross section. It seems that certain substance was filled in PPy matrix and the superposed molecule chains were separated after 400 cycles. The change of thickness seems to be attributed to the fill of certain substance in PPy matrix. Therefore, it is necessary to explore the change of PPy composition during the redox process. Fernández Romero et al.[25] investigated the electrochemical behavior of polypyrrole/poly(vinyl sulfonate) (PPy/PVS) films in acetonitrile containing 0.1 M $LiClO_4$ by the in situ Fourier transform infrared technique. They considered that solvated Li^+ cations can be inserted into the polymeric matrix and formed Li-PVS ionic pairs, which were stabilized and force ClO_4^- as the doping/dedoping ion in the subsequent redox processes. Therefore, when PPy films worked in 1 M EtMeImBF$_4$/PC, the $EtMeIm^+$ cations can be inserted and form ionic pairs, i.e. salt of EtMeImPTS in PPy matrix during the redox processes. As shown in Figure 4, the distance between PPy molecular chains would increase when the salts continuously accumulated among PPy molecular chains, which resulted in the increase of film thickness. The salt can first fill in the grooves on the surface of PPy films, which induced the formation of a homogeneous and smoother surface after 400 cycles. It is noted that the salts in PPy matrix can make the electron transport between PPy molecular chains more difficult. The decrease of electronic conductivity may be correlated with the accumulation of salts in PPy matrix. It is inevitable that molecular structure, surface morphology, thickness and composition of PPy films change when salt continuously accumulates in PPy matrix.

Figure 5 shows the FTIR spectra of PPy films. Two kinds of PPy films have the characteristic peaks of 1630 cm^{-1} (C═C stretching vibration), 1550 cm^{-1} (C−N stretching vibration).[11] The peaks at 2969, 2877, 2924, and 2852 cm^{-1} of PPy films are assigned to $-CH_3$ asymmetric stretch vibration, $-CH_3$ symmetric stretch vibration, $-CH_2-$ asymmetric stretch vibration and $-CH_2-$ symmetric stretch vibration, respectively.[11] Note that the peak at 1030 cm^{-1} of PPy films after 400 cycles was obviously enhanced. This should be related to the BF_4^- asymmetric stretch vibration.[26] The peak at 916 cm^{-1} should be attributed to the CNC stretch vibration at imidazole ring.[27] The H stretch vibration at imidazole ring shows two weak characteristic peaks at 3118 and 3152 cm^{-1}.[26] PPy films had been cleaned carefully by organic solvent and water before FTIR test, and thus the salt of EtMeImBF$_4$ monitored by FTIR test should be in PPy matrix. The filler in PPy matrix which

dx.doi.org/10.1021/jp4054428 | J. Phys. Chem. B 2014, 118, 1353−1362

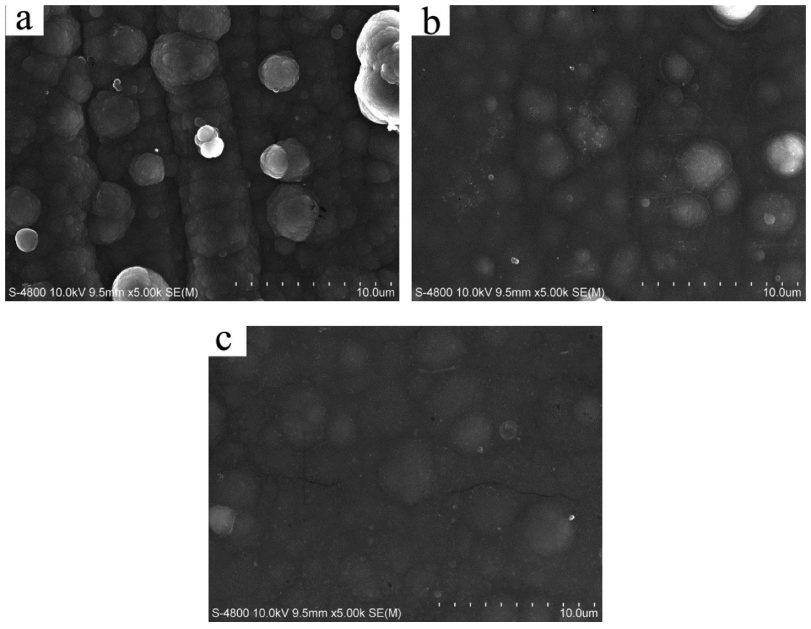

Figure 2. Surface morphology of (a) as-prepared PPy films, (b) PPy films after 50 cycles, and (c) PPy films after 400 cycles in 1 M $EtMeImBF_4$/PC.

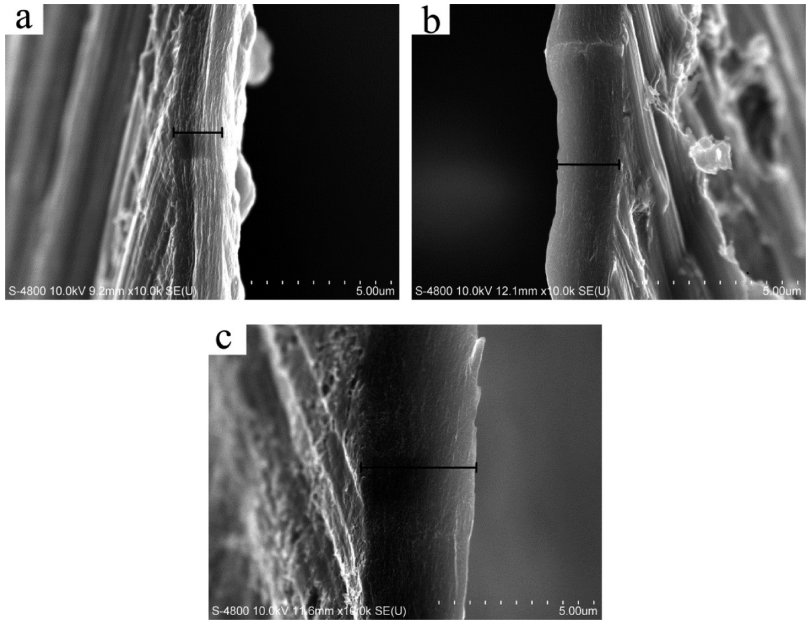

Figure 3. Cross section of (a) as-prepared PPy films, (b) PPy films after 50 cycles, and (c) PPy films after 400 cycles in 1 M $EtMeImBF_4$/PC.

change the cross section morphology and thickness of PPy films must include the salt of $EtMeImBF_4$.

In general, the protonation level on the nitrogen site for PPy films has an important effect on the conductivity and capacitance of PPy films.[28,29] Figure 6 presents the nitrogen 1s (N 1s) XPS core level spectrum of PPy films. These core level spectra of PPy films show relatively broad peaks, indicating the existence of several structures.[28] The decomposed peaks of N 1s at 398.3 ± 0.1, 399.95 ± 0.1, 401.1 ± 0.1, and 402.4 ± 0.2 should be attributed to quinonoid imine (═N−), benzenoid amine (−NH−), protonation benzenoid amine ($-NH^+-$) and protonation quinonoid imine ($=NH^+-$), respectively.[28−30] The quinonoid imine structure is used to estimate the density of defect in PPy matrix.[12,28] The spectra of the as-prepared PPy films did not show the peak of quinonoid imine, indicating that the PPy prepared at low temperatures has few defects.[31] The spectrum of PPy films after 50 cycles shows a strong peak of quinonoid imine at 398.4. The decrease of the protonation level of PPy films in Figure 6b should be attributed to the peak of quinonoid imine. In Figure 6c, the protonation level of PPy films continued to decrease with the increase of cyclic number and decreased to 21.3% after 400 cycles. The N 1s shoulder on the higher energy side, which results from an electrostatic effect of the nearest counterion,[28] became relatively weak for PPy films after 400 cycles. This should be the main reason for the sharp decrease of protonation level for PPy films. The rapid decrease of PPy conductivity and discharge capacitance should be closely related to the sharp decrease of PPy protonation level.

dx.doi.org/10.1021/jp4054428 | J. Phys. Chem. B 2014, 118, 1353−1362

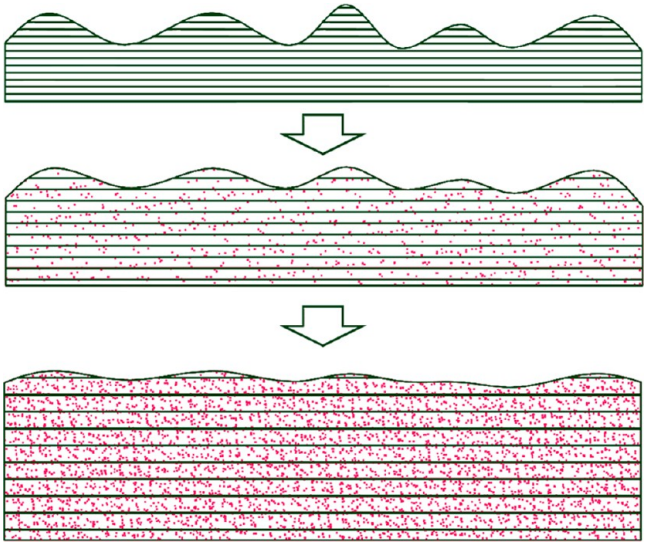

Figure 4. Scheme for the change of the cross section of PPy films in 1 M $EtMeImBF_4$/PC.

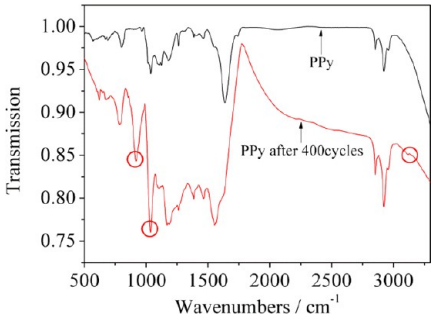

Figure 5. FTIR spectra of PPy films.

EQCM is an ideal tool for the study of compositional changes that occur during the redox process in thin films of conducting polymers.[16,32−36] In order to explain the ions doping/dedoping behavior in 1 M $EtMeImBF_4$/PC, EQCM measurements were carried out to monitor the mass changes of PPy films associated with the redox process. The simplified Sauerbrey equation for mass change on a thin film can be described by following eq 1

$$\Delta f = -2f_0^{\,2}\,\Delta m/A(\mu_q\rho_q)^{1/2} \quad (1)$$

where Δf is the measured frequency shift, f_0 the frequency of the quartz crystal prior to a mass change, Δm the mass change, A the piezoelectrically active area, ρ_q the density of quartz, and μ_q the shear modulus.

Figure 7 shows the mass change of PPy films monitored by EQCM during corresponding CV scan in 1 M $MeEt_3ImBF_4$/

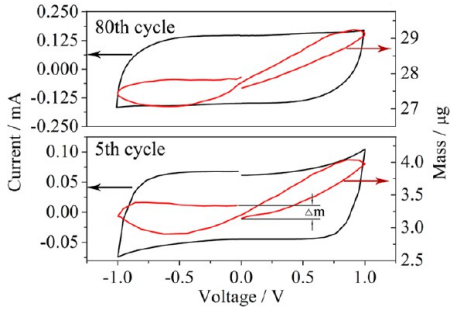

Figure 7. EQCM response of PPy films corresponding to CV scan in 1 M $EtMeImBF_4$/PC.

PC. In the fifth cycle, the mass change of PPy films calculated by charging capacitance from 0 to 1 V was 3.32 μg if the mass change was considered as the insertion of BF_4^- anions from supporting electrolyte. However, the mass change of PPy films

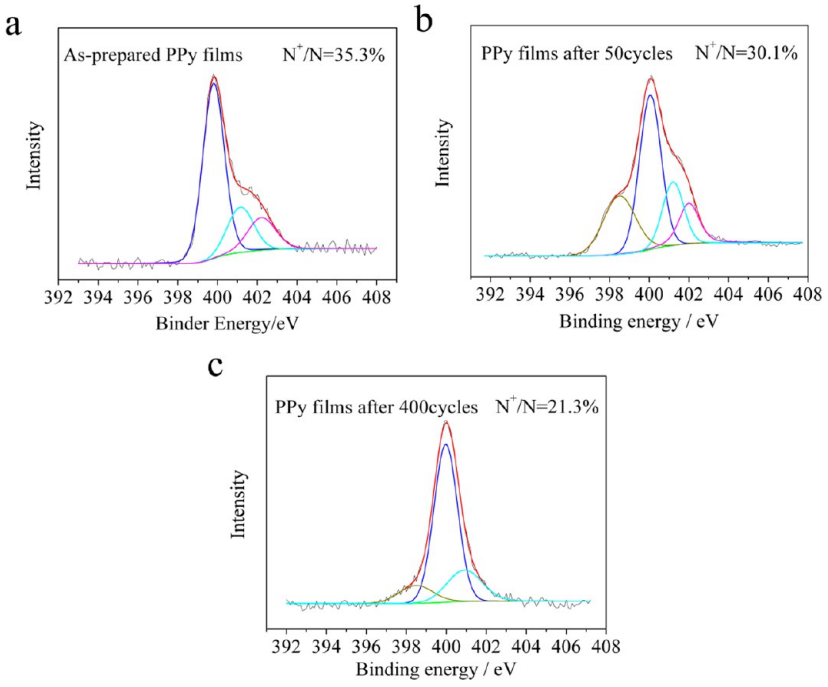

Figure 6. Nitrogen 1s (N 1s) XPS core level spectrum of PPy films: (a) as-prepared PPy films, (b) PPy films after 50 cycles, and (c) PPy films after 400 cycles in 1 M $EtMeImBF_4$/PC.

dx.doi.org/10.1021/jp4054428 | J. Phys. Chem. B 2014, 118, 1353−1362

monitored by EQCM was only 0.85 μg. Therefore, PPy oxidization from 0 to 1 V can be related to both insertion of anions in supporting electrolyte and the ejection of cations in PPy matrix. The ejected cations in this process reduced the mass change of PPy films monitored by EQCM. The cations in PPy matrix derived from previous several cycles. This process can be described by following eq 2:

$$\mathrm{PPy}^{n+}\cdot\mathrm{PTS}^{(n+a)-}\cdot\mathrm{EtMeIm}^{a+} - b\mathrm{e}^{-} + (b-c)\mathrm{BF_4}^{-} - c\mathrm{EtMeIm}^{+} \xrightarrow{\text{oxidation}} \mathrm{PPy}^{(n+b)+}\cdot\mathrm{PTS}^{(n+a)-}\cdot\mathrm{BF_4}^{(b-c)-}\cdot\mathrm{EtMeIm}^{(a-c)+} \quad (2)$$

It is obvious that the insertion of anions were more than ejection of cations. The mass difference between insertion of anions and ejection of cations was 0.85 μg. The solvent molecules can insert during the oxidation process, which can result in a certain increase of PPy mass. The mass of the PPy films decreased with the decrease of the cell voltage from 1 V to −0.5 V. If the reduction process from 1 V to −0.5 V was attributed to the ejection of BF_4^-, the mass change of PPy films calculated by discharging capacitance was 2.34 μg. The mass change of PPy films monitored by EQCM was only 1.07 μg. Therefore, the cations can insert from supporting electrolyte when BF_4^- anions was ejected, which can be described by following eq 3:

$$\mathrm{PPy}^{(n+b)+}\cdot\mathrm{PTS}^{(n+a)-}\cdot\mathrm{BF_4}^{(b-c)-}\cdot\mathrm{EtMeIm}^{(a-c)+} + (b+d)\mathrm{e}^{-} - i\mathrm{PTS}^{-} - (j+c)\mathrm{BF_4}^{-} + (c+k)\mathrm{EtMeIm}^{+} \xrightarrow{\text{Reduction}} \mathrm{PPy}^{(n-d)+}\cdot\mathrm{PTS}^{(n+a-i)-}\cdot\mathrm{BF_4}^{(b-j)-}\cdot\mathrm{EtMeIm}^{(a+k)+} \quad (3)$$

The ejected anions should be more than the inserted cations. The mass difference between ejection of anions and insertion of cations was 1.07 μg. On the other hand, some solvent molecules can be ejected during the oxidation process. The mass of the PPy films increased during further reduction process from the cell voltage of −0.5 to −1 V, which was only explained by more $EtMeIm^+$ cations inserting from supporting electrolyte because the anions cannot be inserted in the reduction process. This oxidation process is similar to that described by eq 3, however, the inserted cations become more than the ejected anions, which can be described by following eq 4:

$$\mathrm{PPy}^{(n-d)+}\cdot\mathrm{PTS}^{(n+a-i)-}\cdot\mathrm{BF_4}^{(b-j)-}\cdot\mathrm{EtMeIm}^{(a+k)+} + d_1\mathrm{e} - i_1\mathrm{PTS}^{-} - j_1\mathrm{BF_4}^{-} + k_1\mathrm{EtMeIm}^{+} \xrightarrow{\text{reduction}} \mathrm{PPy}^{(n-d-d_1)+}\cdot\mathrm{PTS}^{(n+a-i-i_1)-}\cdot\mathrm{BF_4}^{(b-j-j_1)-}\cdot\mathrm{EtMeIm}^{(a+k+k_1)+} \quad (4)$$

The mass difference between ejection of anions and insertion of cations was 0.27 μg according to the EQCM result. Some solvent molecules can be ejected during the oxidation process. The mass change of PPy films is small when PPy films were oxidized again from the cell voltage of −1 V to 0 V. This indicates that the $EtMeIm^+$ cations which had been inserted during the reduction process were not ejected completely. The detained $EtMeIm^+$ cations can bond with anions in PPy matrix, which resulted in the increase of PPy mass in Figure 7, i.e., Δm. Otero et al. found a weight increase when PPy films were worked in 0.1 M $LiClO_4$ aqueous solution.[7] Fernández Romero et al.[25] considered that the protonation level on the nitrogen site of PPy films did not change though the solvated Li^+ cations can be inserted into the polymeric matrix and form Li−PVS ionic pairs when PPy films worked in acetonitrile containing 0.1 M $LiClO_4$. However, the rapid decrease of protonation level in Figure 6 indicated that the combination of retained $EtMeIm^+$ cations with the doped anions in PPy matrix can occur in every cycle. Therefore, the oxidation of PPy films from the cell voltage of −1 V to 0 V can be described by following eq 5:

$$\mathrm{PPy}^{(n-d-d_1)+}\cdot\mathrm{PTS}^{(n+a-i-i_1)-}\cdot\mathrm{BF_4}^{(b-j-j_1)-}\cdot\mathrm{EtMeIm}^{(a+k+k_1)+} - (d_2-d-d_1)\mathrm{e}^{-} + (i+i_1-i_2)\mathrm{PTS}^{-} + (j+j_1-j_2)\mathrm{BF_4}^{-} - (k+k_1-k_2)\cdot\mathrm{EtMeIm}^{+} \xrightarrow{\text{oxidation}} \mathrm{PPy}^{(n-d_2)+}\cdot\mathrm{PTS}^{(n+a-i_2)-}\cdot\mathrm{BF_4}^{(b-j_2)-}\cdot\mathrm{EtMeIm}^{(a+k_2)+} \quad (5)$$

where $n - d_2 + a + k_2 = n + a - i_2 + b - j_2$, *i.e.*, $k_2 - d_2 = b - i_2 - j_2$ due to the electric neutrality in PPy matrix. The value of d_2 in eq 5 should increase in later cycles because the protonation level of PPy films rapidly decreased with the increase of cyclic number. Moreover, the value of k_2 in eq 5 should increase in later cycles, which indicated the accumulation of salt in PPy matrix and increase of film thickness.

As shown in Figure 7, the curves of mass change in eightieth cycle is similar that in the fifth cycle, indicating that the ions insertion/ejection process cannot change in latter cycle. Both of cations and anions in supporting electrolyte participated in the redox process of PPy films. Moreover, the mass of PPy films continued to increase during later every cycle, which resulted in the continuous increase of film thickness in Figure 3. The mass of PPy films on gold electrode increased by 27.1 μg after 80 cycles. Table 2 shows the molar ratio of carbon and nitrogen from the wide scan XPS spectra of PPy films. The molar ratio of C/N decreased from 9.1:1 to 6.0:1 during the degradation process of PPy films, which should be related to the detained $EtMeIm^+$ cations in PPy matrix due to the low content of nitrogen in $EtMeIm^+$ cations compared to that in PPy matrix.

Table 2. Molar Ratio of Carbon and Nitrogen from the Wide Scan XPS Spectra of PPy Films

PPy films	C/N
as-prepared PPy films	9.1:1
PPy films after 50 cycles	7.1:1
PPy films after 400 cycles	6.0:1

As shown in Figure 8, PPy is one of the p-type (hole transporting) conducting polymers.[37] The spatially localized counterions are incorporated into PPy matrix by electrostatic pinning. However, the $EtMeIm^+$ cations in supporting electrolyte were inserted into PPy matrix during the reduction process and formed salts in PPy matrix. The increase of film thickness observed by FESEM should be attributed to the continuous accumulation of salts in PPy matrix. The rapid decrease of the protonation level on the nitrogen site for PPy films confirmed that the retained $EtMeIm^+$ cations can neutralize some doped anions in PPy matrix and formed salts. The doped anions of PPy film was neutralized by the cations from supporting electrolyte, which should results in the formation of compensate semiconductor state in PPy matrix.

Figure 8 shows the formation process of the compensate semiconductor state in PPy matrix. During the charge/discharge process of PPy films in 1 M $EtMeImBF_4$/PC, the

dx.doi.org/10.1021/jp4054428 | J. Phys. Chem. B 2014, 118, 1353−1362

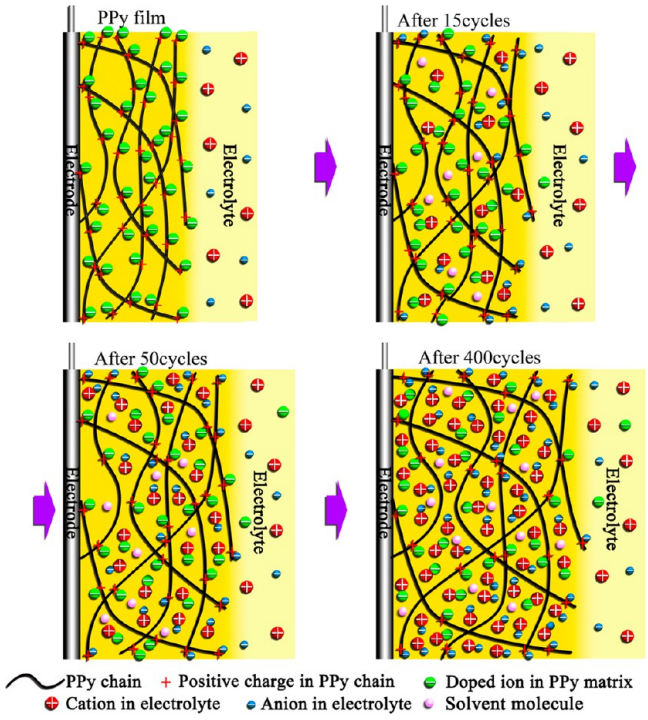

Figure 8. Scheme of formation process for the compensate semiconductor state in PPy matrix.

doped ion of PTS^- anions was partly substituted by BF_4^- anions from supporting electrolyte. The doped ions in outer layer of PPy films were easily substituted by BF_4^- anions compared with that in inner layer of PPy films. The thickness of PPy films continuously increased with the increase of cyclic number when the retained $EtMeIm^+$ cations banded with doped PTS^- anions in PPy matrix or BF_4^- anions from supporting electrolyte and formed salts in PPy matrix. A small amount of PTS^- anions were ejected into supporting electrolyte during oxidation process. The free volume in PPy matrix obviously decreased after 400 cycles due to the accumulation of the salts, though the distance between PPy molecule chains increased during PPy redox process. In addition, some solvent molecules can retain in PPy matrix during redox process. The result for combination of different ions in PPy matrix can be described by eq 6:

$$PPy^{n+}\cdot PTS^{n-} \xrightarrow{\text{after 400 cycles}} PPy^{(n-u)+}\cdot PTS^{(n-u-v)-}\cdot BF_4^{v-}\cdot x(BMIm^+\cdot PTS^-)\cdot y(BMIm^+\cdot BF_4^-) \quad (6)$$

where $u = i_1 + i_2 + i_3 + ... + i_{400}$ (i_n represents the decrease of the protonation level on the nitrogen site for PPy films in every cycle). Charges on PPy chains reduced from n to $n - u$ due to combination of doped anions with $EtMeIm^+$ cations from supporting electrolyte, *i.e.* the formation of the compensate semiconductor state in PPy matrix. Meanwhile, two kinds of salts including EtMeImPTS and $EtMeImBF_4$ were formed in PPy matrix during PPy redox process.

As shown in Figure 8, there is small amount of salts in PPy matrix after 15 cycles. Malcolm et al.[38] prepared PPy films containing polysulfonated aromatic anions with good capacitive response. They considered that polysulfonated aromatic anions with big size in PPy matrix open the channels in which fast ionic motion can occurs. Therefore, small amount of salts in PPy matrix can open more channels for the entry of ions from the supporting electrolyte, which resulted in more active material participating in the ions doping/dedoping process. This should be the main reason for the very high specific capacitance of PPy films after 15 cycles. However, the opened channels were gradually blocked by the continuously accumulated salts in PPy matrix. The structure of PPy films after 400 cycles became more compact and closed than that of as-prepared PPy films. We found that PPy films after 400 cycles were more brittle and easy to crack when they were dried.

The change of PPy structure should affect the internal resistance of PPy films. EIS is used to study for the electrochemical behavior of conducting polymers, especially for the relation of electrochemical behavior with the structure of conducting polymers.[11,16,28,36,39−41] Theoretical models of conducting polymers have been broadly discussed in the literature.[16,39−42] Figure 9a shows the basic scheme for these

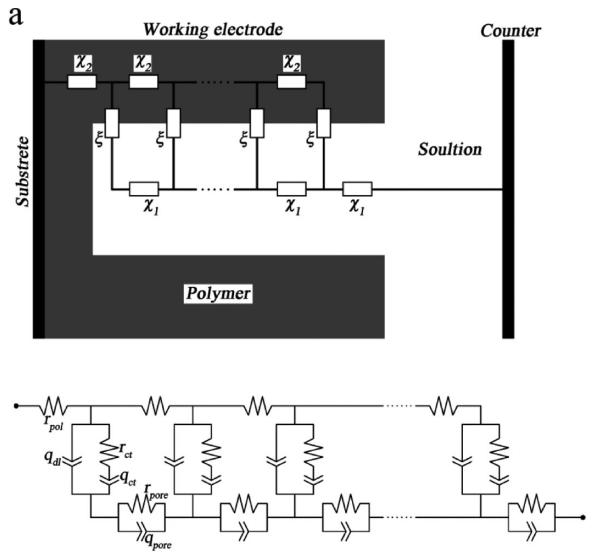

Figure 9. (a) Scheme of a generic porous electrode. (b) Model for a physical description of ions doping/dedoping process in PPy matrix.

models. The quantities χ_1 and χ_2 are impedances per unit length ($\Omega\cdot m^{-1}$) transverse to the macroscopic outer surfaces, corresponding to the whole electrode area. On the other hand, ξ is an impedance length ($\Omega\cdot m$) parallel to the macroscopic surfaces, describing faradaic currents and polarization at the distributed interface. However, the model of the electrode behavior in its reduced state or near the insulator to conductor transition maybe a mixed (both electronic and ionic) conduction but not a simple phase. When transport features in both phases yield comparable behavior, it is often difficult to interpret experimental data unambiguously. In this case, the elements χ_1 and χ_2 may not correspond to simple resistive responses.[40]

Msrchesi et al.[16] investigated PPy degradation using EIS and proposed a model for PPy electrode, which is shown in Figure 9b. In this model, r_{pol} represents the polymer resistance, which corresponds to χ_2 in Figure 9a. The ions diffusion in the pores of PPy surface is represented by r_{pore} and q_{pore}, which corresponds to χ_1 in Figure 9a. The polymer/solution interface ζ in Figure 9a is represented by a double-layer capacitance (q_{dl}) in parallel with the charge transfer resistance (r_{ct}), which is in series with the charge-transfer capacitance (q_{ct}). q_{pore}, q_{dl}, and q_{ct} were represented by the constant phase element (CPE) with fractional exponent of n. The CPE has been considered to

dx.doi.org/10.1021/jp4054428 | J. Phys. Chem. B 2014, 118, 1353−1362

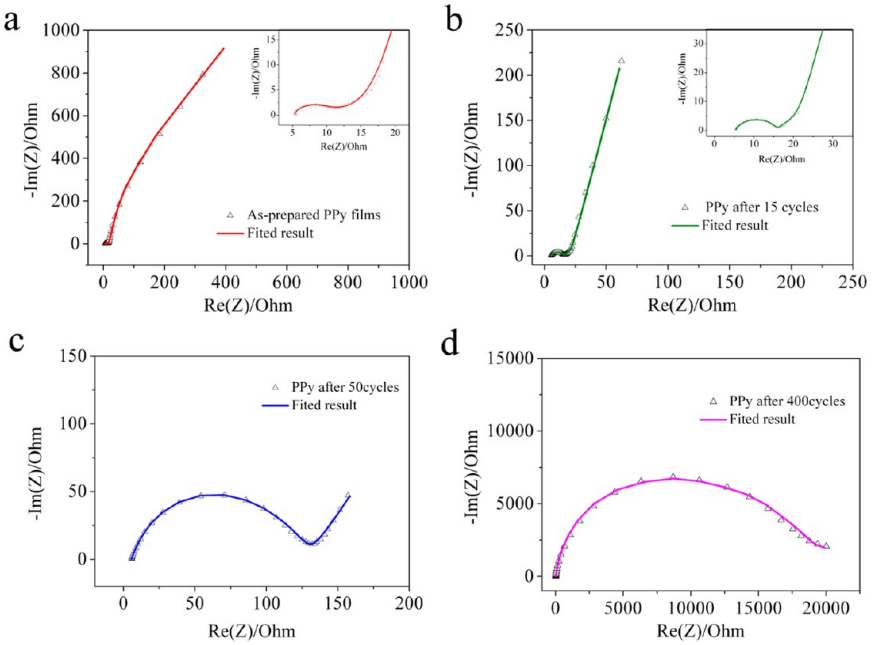

Figure 10. Nyquist plot and fitted result of (a) as-prepared PPy films, (b) PPy films after 15 cycles, (c) PPy films after 50 cycles, and (d) PPy films after 400 cycles.

represent a circuit parameter with limiting behavior as a capacitor for $n = 1$, a resistor for $n = 0$, and an inductor for $n = -1$.[43] The good fit quality was obtained using this model. As shown in Figure 10, there is a very good adjustment between the experimental data and calculated data.

Table 3 shows the parameter values of PPy films in different degradation stage using the transmission line model in Figure 9b. The calculated parameters of r_{ct} and r_{pore} change greatly during the degradation process of PPy films. This should be related to the change of PPy structure. The r_{pore} value of as-prepared PPy films was big, which can be attributed to poor wettability in pores of PPy films surface. We found that the r_{pore} value decrease with the increase of standing time. The r_{pore} value decreased more rapidly when PPy films worked in $EtMeImBF_4$/PC. The electric field force on the interface of PPy films can promote the electrolyte penetrating into the pores on the surface. On the other hand, small amount of salts in PPy matrix can open the channels for the entry of ions. Therefore, the value of r_{pore} shows a huge decrease after 15 cycles. However, the r_{pore} value increased markedly in latter cycle and reached 6571 Ωcm^{-1} after 400 cycles. The continuous accumulation of the salts during the redox process not only blocked ions insertion/ejection but also occupied much free volume in PPy matrix. The decrease of PPy free volume should result in a compact and closed polymer structure. The pore size on the PPy surface can reduce with the increase of salt in PPy matrix. The continuous reduction of pore diameter can cause a huge increase of r_{pore} value from the 16th to the 400th cycle.

Table 3. Parameter Values of PPy Films in Different Degradation Stage Using the Transmission Line Model in Figure 8b

	0 cycle	after 15 cycles	after 50 cycles	after 400 cycles
$(r_{pol}/r_{pol})/\Omega\ cm^{-1}$	4.95	5.23	5.43	6.45
$q_{dl}/10^{-6}\ F\ s^{n-1}\ cm^{-1}$	2.49	3.83	3.99	5.63
n_{dl}	0.77	0.78	0.72	0.80
$r_{ct}/\Omega\ cm^{-1}$	4.03	10.69	77.54	12 897.73
$q_{ct}/10^{-4}\ F\ s^{n-1}\ cm^{-1}$	0.02	525.05	30.23	2.68
n_{ct}	0.20	0.92	0.64	0.64
$q_{pore}/10^{-4}\ F\ s^{n-1}\ cm^{-1}$	99.35	78.22	0.19	0.25
n_{pore}	0.95	0.70	0.99	0.99
$r_{pore}/\Omega\ cm^{-1}$	2652.15	5.29	77.54	6571.42

The r_{ct} value increased by 4 orders of magnitude after 400 cycles. The insertion/ejection of ions on PPy surface must accompany with conformational changes of PPy chains.[19,44] The free volume in PPy matrix provides space for conformational changes of PPy chains.[19,44] The decrease of free volume in PPy matrix due to the accumulation of salts can make conformational changes of PPy chains more difficult. Therefore, the insertion/ejection of ions on PPy surface became more difficult due to the reduction of free volume, which should be main reason for the marked increase of r_{ct} value. The elimination of salt formation in PPy matrix should reduce the internal resistance and improve the stability of PPy films. In addition, n_{ct} varied very big after 15 cycles. PPy films have a poor wettability in 1 M $EtMeImBF_4$/PC. Therefore, a little supporting electrolyte permeated into PPy matrix before cell cycling. The electrochemical behavior of PPy films before cell cycling is more like a resistor and n_{ct} should be small. After 15 cycles, a lot of supporting electrolyte permeated into PPy matrix. Small amount of salts in PPy matrix can open more channels of ion insertion and resulted in a very high capacitance after 15 cycles. The electrochemical behavior of PPy films after 15 cycles is more like a capacitor and n_{ct} should became bigger than that before cell cycling.

The compensate semiconductor effect in PPy matrix can occur in various electrolyte, which should influence the rate of PPy degradation during redox process. The size of ions in electrolyte should have an important effect on the compensate semiconductor effect in PPy matrix. In our previous studies,[11,22] it seems that the compensate semiconductor effect did not occur in PPy matrix when PPy films worked in HCl aqueous

dx.doi.org/10.1021/jp4054428 | J. Phys. Chem. B 2014, 118, 1353−1362

solution. The size of H^+ ions is small compared with that of $EtMeIm^+$ cations, so H^+ ions which have been inserted during reduction process can be ejected during oxidation process. This should be one of main reason for good stability of PPy films in HCl aqueous solution. Therefore, the small size of cations in electrolyte should contribute to the elimination of compensate semiconductor effect in PPy matrix.

4. CONCLUSION

The cations in supporting electrolyte played an important role when PPy films worked in 1 M $EtMeImBF_4$/PC. EQCM result indicated that $EtMeIm^+$ cations retained in PPy matrix and formed salts due to the combination of $EtMeIm^+$ cations with doped PTS^- anions and BF_4^- anions from supporting electrolyte. A little of salts in PPy matrix can increase channels for ions insertion during doping/dedoping process. More active material can participate in ions doping/dedoping process, which resulted in a very high specific capacitance of 420 $F{\cdot}g^{-1}$ after 14 cycles.

The protonation level on the nitrogen site for PPy films rapidly decayed due to the continuous combination of detained $EtMeIm^+$ cations with dope anion of PTS^-, which induced the formation of compensate semiconductor state in PPy matrix. The occurrence of compensate semiconductor effect in PPy matrix should be one of main reasons for the rapid decay of PPy electronic conductivity and specific capacitance. The thickness of PPy films increased by two times after 400 cycles due to the continuous accumulation of salts. The free volume in PPy matrix can decrease due to the continuous accumulation of salts. The great increase of PPy internal resistance after 400 cycles should be closely correlated to the decrease of free volume in PPy matrix.

The compensate semiconductor effect in PPy matrix can occur in various electrolyte. The small size of cations in supporting electrolyte can contribute to the elimination of compensate semiconductor effect in PPy matrix.

■ ASSOCIATED CONTENT

Ⓢ Supporting Information

3D surface morphology of PPy films examined by optical microscope, the decay process of PPy films in $EtMeImBF_4$/ACN, and the mass change of PPy films in three electrodes system. This material is available free of charge via the Internet at http://pubs.acs.org.

■ AUTHOR INFORMATION

Corresponding Authors

*E-mail: (J.P.W.) wangjingping@sust.edu.cn. Telephone: 0086-029-86168135.

*E-mail: (Y.X.) ylxu@mail.xjtu.edu.cn.

Author Contributions

§These authors contributed equally.

Notes

The authors declare no competing financial interest.

■ ACKNOWLEDGMENTS

The authors wish to express thanks for the financial support by the Natural Science Basic Research Plan in Shaanxi Province of China (Grant No. 2011JM6003), the Specialized Research Fund for the Doctoral Program of Higher Education of China (Grant No. 20110201130005), Program for New Century Excellent Talents in University (NCET-11-0433), Doctor Startup Fund of Shaanxi University of Science and Technology (Grant No. BJ12-05), and National Natural Science Foundation of China (Grant No. 21274115).

■ REFERENCES

(1) Jager, E. W. H.; Smela, E.; Inganas, O. Inganas, Microfabricating conjugated polymer actuators. *Science* **2000**, *290*, 1540−1545.

(2) Frackowiak, E.; Khomenko, V.; Jurewicz, K.; Lota, K.; Beguin, F. Supercapacitors based on conducting polymers/nanotubes composites. *J. Power Sources* **2006**, *153*, 413−418.

(3) Mirfakhrai, T.; Madden, J. D. W.; Baughman, R. H. Polymer artificial muscles. *Mater. Today* **2007**, *10*, 30−38.

(4) Sadki, S.; Schottland, P.; Brodie, N.; Sabouraud, G. The mechanisms of pyrrole electropolymerization. *Chem. Soc. Rev.* **2000**, *29*, 283−293.

(5) Schlenoff, J. B.; Xu, H. Evolution of Physical and Electrochemical Properties of Polypyrrole during Extended Oxidation. *J. Electrochem. Soc.* **1992**, *139*, 2397−2401.

(6) Chehimi, M. M.; Abdeljalil, E. A study of the degradation and stability of polypyrrole by inverse gas chromatography, X-ray photoelectron spectroscopy, and conductivity measurements. *Synth. Met.* **2004**, *145*, 15−22.

(7) Otero, T. F.; Marquez, M.; Suarez, I. J. Polypyrrole: Diffusion Coefficients and Degradation by Overoxidation. *J. Phys. Chem. B* **2004**, *108*, 15429−15433.

(8) Moss, B. K.; Burford, R. P. A kinetic study of polypyrrole degradation. *Polymer* **1992**, *33*, 1902−1908.

(9) Jurewicz, K.; Delpeux, S.; Bertagna, V.; Beguin, F.; Frackowiak, E. Supercapacitors from nanotubes/polypyrrole composites. *Chem. Phys. Lett.* **2001**, *347*, 36−40.

(10) Sharma, R. K.; Rastogi, A. C.; Desu, S. B. Pulse polymerized polypyrrole electrodes for high energy density electrochemical supercapacitor. *Electrochem. Commun.* **2008**, *10*, 268−272.

(11) Wang, J.; Xu, Y.; Wang, J.; Du, X.; Xiao, F.; Li, J. High charge/discharge rate polypyrrole films prepared by pulse current polymerization. *Synth. Met.* **2010**, *160*, 1826−1831.

(12) Wang, J.; Xu, Y.; Zhu, J.; Ren, P. Electrochemical in situ polymerization of reduced graphene oxide/polypyrrole composite with high power density. *J. Power Sources* **2012**, *208*, 138−143.

(13) Debiemme-Chouvy, C.; Tran, T. T. M. An insight into the overoxidation of polypyrrole materials. Electrochem. Commun. *Electrochem. Commun.* **2008**, *10*, 947−950.

(14) Cataldo, F.; Omastova, M. Polym. On the ozone degradation of polypyrrole. *Degrad. Stab.* **2003**, *82*, 487−495.

(15) Cheah, K.; Forsyth, M.; Truong, V. T. Ordering and stability in conducting polypyrrole. *Synth. Met.* **1998**, *94*, 215−219.

(16) Marchesi, L. F. Q. P.; Simoes, F. R.; Pocrifka, L. A.; Pereira, E. C. Investigation of Polypyrrole Degradation Using Electrochemical Impedance Spectroscopy. *J. Phys. Chem. B* **2011**, *115*, 9570−9575.

(17) Bull, R. A.; Fan, F.-R. F.; Bard, A. J. Polymer Films on Electrodes VII. Electrochemical Behavior at Polypyrrole-Coated Platinum and Tantalum Electrodes. *J. Electrochem. Soc.* **1982**, *129*, 1009−1015.

(18) Beck, F.; Braun, P.; Oberst, M. Bunsenges Ber. Organic electrochemistry in the solid state overoxidation of polypyrrole. *Phys. Chem.* **1987**, *91*, 967−974.

(19) Otero, T. F.; Grande, H.-J.; Rodríguez, J. Reinterpretation of polypyrrole electrochemistry after consideration of conformational relaxation processes. *J. Phys. Chem. B* **1997**, *101*, 3688−3697.

(20) Rodríguez, I.; Scharifker, B. R.; Mostany, J. In situ FTIR study of redox and overoxidation processes in polypyrrole films. *J. Electroanal. Chem.* **2000**, *491*, 117−125.

(21) Li, Y.; Qian, R. Electrochemical overoxidation of conducting polypyrrole nitrate film in aqueous solutions. *Electrochim. Acta* **2000**, *45*, 1727−1731.

(22) Wang, J.; Xu, Y.; Wang, J.; Du, X. Toward a high specific power and high stability polypyrrole supercapacitors. *Synth. Met.* **2011**, *161*, 1141−1144.

(23) Pringle, J. M.; Efthimiadis, J.; Howlett, P. C.; Efthimiadis, J.; MacFarlane, D. R.; Chaplin, A. B.; Hall, S. B.; Officer, D. L.; Wallace, G. G.; Forsyth, M. Electrochemical synthesis of polypyrrole in ionic liquids. *Polymer* **2004**, *45*, 1447−1453.
(24) Snook, G. A.; Kao, P.; Best, A. S. Conducting-polymer-based supercapacitor devices and electrodes. *J. Power Sources* **2011**, *196*, 1−12.
(25) Fernandez Romero, A. J.; Lopez Cascales, J. J.; Otero, T. F. In Situ FTIR Spectroscopy Study of the Break-In Phenomenon Observed for PPy/PVS Films in Acetonitrile. *J. Phys. Chem. B* **2005**, *109*, 21078−21085.
(26) Katsyuba, S. A.; Zvereva, E. E.; Vidis, A.; Dyson, P. J. Application of density functional theory and vibrational spectroscopy toward the rational design of ionic liquids. *J. Phys. Chem. A* **2007**, *111*, 352−70.
(27) Watts, H. D.; Archibald, D. D.; Mohamed, M. N. A.; Kubicki, J. D. In search of OH-pi interactions between 1-methylimidazole and water using a combined computational quantum chemistry and ATR-FTIR spectroscopy approach. *J. Mol. Struct.* **2012**, *1026*, 78−87.
(28) Joo, J.; Lee, J. K.; Lee, S. Y.; Jang, K. S.; Oh, E. J.; Epstein, A. J. Physical characterization of electrochemically and chemically synthesized polypyrroles. *Macromolecules* **2000**, *33*, 5131−5136.
(29) Hu, C. C.; Lin, X. X. Ideally capacitive behavior and X-ray photoelectron spectroscopy characterization of polypyrrole. *J. Electrochem. Soc.* **2002**, *149*, A1049−A1057.
(30) Kang, E. T.; Neoh, K. G.; Ong, Y. K.; Tan, K. L.; Tan, B. T. G. X-ray photoelectron spectroscopic studies of polypyrrole synthesized with oxidative iron(III) salts. *Macromolecules* **1991**, *24*, 2822−2828.
(31) Osagawara, M.; Funahashi, K.; Demura, T.; Hagiwara, T.; Iwata, K. Enhancement of electrical conductivity of polypyrrole by stretching. *Synth. Met.* **1986**, *14*, 61−69.
(32) Bruckenstein, S.; Brzezinska, K.; Hillman, A. R. EQCM studies of polypyrrole films. 1. Exposure to aqueous sodium tosylate solutions under thermodynamically permselective conditions. Electrochim. *Electrochim. Acta* **2000**, *45*, 3801−3811.
(33) Bruckenstein, S.; Brzezinska, K.; Hillman, A. R. EQCM studies of polypyrrole films. Part 2. Exposure to aqueous sodium tosylate solutions under thermodynamically non-permselective conditions. *Phys. Chem. Chem. Phys.* **2000**, *2* (6), 1221−1229.
(34) Weidlich, C.; Mangold, K. M.; Juttner, K. EQCM study of the ion exchange behaviour of polypyrrole with different counterions in different electrolytes. *Electrochim. Acta* **2005**, *50*, 1547−1552.
(35) Syritski, V.; Opik, A.; Forsen, O. Ion transport investigations of polypyrroles doped with different anions by EQCM and CER techniques. Electrochim. *Electrochim. Acta* **2003**, *48*, 1409−1417.
(36) Dziewonski, P. M.; Grzeszczuk, M. Impact of the Electrochemical Porosity and Chemical Composition on the Lithium Ion Exchange Behavior of Polypyrroles (ClO4-, TOS-, TFSI-)Prepared Electrochemically in Propylene Carbonate. Comparative EQCM, EIS and CV Studies. *J. Phys. Chem. B* **2010**, *114*, 7158−7171.
(37) Chen, X. L.; Jenekhe, S. A. Bipolar conducting polymers: Blends of p-type polypyrrole and an n-type ladder polymer. *Macromolecules* **1997**, *30*, 1728−1733.
(38) Ingram, M. D.; Staesche, H.; Ryder, K. S. 'Ladder-doped' polypyrrole: a possible electrode material for inclusion in electrochemical supercapacitors? *J. Power Sources* **2004**, *129*, 107−112.
(39) Paasch, G.; Micka, K.; Gersdorf, P. Theory of the electrochemical impedance of macrohomogeneous porous electrodes. *Electrochim. Acta* **1993**, *38*, 2653−2662.
(40) Garcia-Belmonte, G.; Bisquert, J.; Pereira, E. C.; Fabregat-Santiago, F. Switching behaviour in lightly doped polymeric porous film electrodes. Improving distributed impedance models for mixed conduction conditions. *J. Electroanal. Chem.* **2001**, *508*, 48−58.
(41) Garcia-Belmonte, G.; Bisquert, J. Impedance analysis of galvanostatically synthesized polypyrrole films. Correlation of ionic diffusion and capacitance parameters with the electrode morphology. *Electrochim. Acta* **2002**, *47*, 4263−4272.
(42) Raistrick, I. D. Impedance studies of porous electrodes. *Electrochim. Acta* **1990**, *35*, 1579−1586.
(43) Jorcin, J. B.; Orazem, M. E.; Pebere, N.; Tribollet, B. CPE Analysis by Local Impedance Spectroscopy. *Electrochim. Acta* **2006**, *51*, 1473−1479.
(44) Otero, T. F.; Angulo, E. Oxidation-reduction of polypyrrole films. Kinetics, structural model and applications. *Solid State Ionics* **1993**, *63*−*65*, 803−809.